GFD 2013 Lecture 8: Rotating currents

Paul Linden; notes by Dhruv Balwada & Ton van den Bremer

June 26, 2013

1 Introduction

Figure 1 shows two examples of gravity currents occurring on the earth's surface in the direct vicinity of boundaries. Rotation has the important effect of adding a Coriolis force to the momentum equations in the non-inertial rotating frame of reference. Under the influence of the Coriolis force, currents travelling to the North on the Northern hemisphere will deviate to the east, as will currents travelling to the South on the Southern hemisphere. These currents will follow or even curve around the land boundaries they meet on their paths. In this lecture, the effect of the Coriolis force on light gravity currents is explored in the context of shallow water theory.

Figure 2 shows an example from a lab experiment. A shallow cylindrical lens of light water is released at the centre of a rotating tank on top of a thick layer of dense water. The tank rotates in the clockwise direction. As some of the light fluid spreads radially upon release, it must start rotating in the anti-clockwise direction to conserve angular momentum to simulate the effect of a land boundary. A solid radial boundary is then introduced that prevents flow in the azimuthal direction across the entire depth of the fluid. The presence of the radial boundary blocks the azimuthal flow, and the current propagates along the radial boundary in the radially outward direction under the influence of the Coriolis force in the same way as gravity currents observed in real life might do along a coastline (cf. figure 1).

2 Light boundary currents: shallow water theory

We consider a gravity current with thickness h in a reference frame rotating around the z axis, the axis along which gravity g acts in the negative direction, at angular velocity Ω, as illustrated in figure 3. Its dynamics are described by shallow water theory, and conservation of momentum in the x, y and z direction give:

$$u_t + uu_x + vu_y - fv = -\frac{1}{\rho_0}p_x, \tag{1}$$

$$v_t + uv_x + vv_y + fu = -\frac{1}{\rho_0}p_y, \tag{2}$$

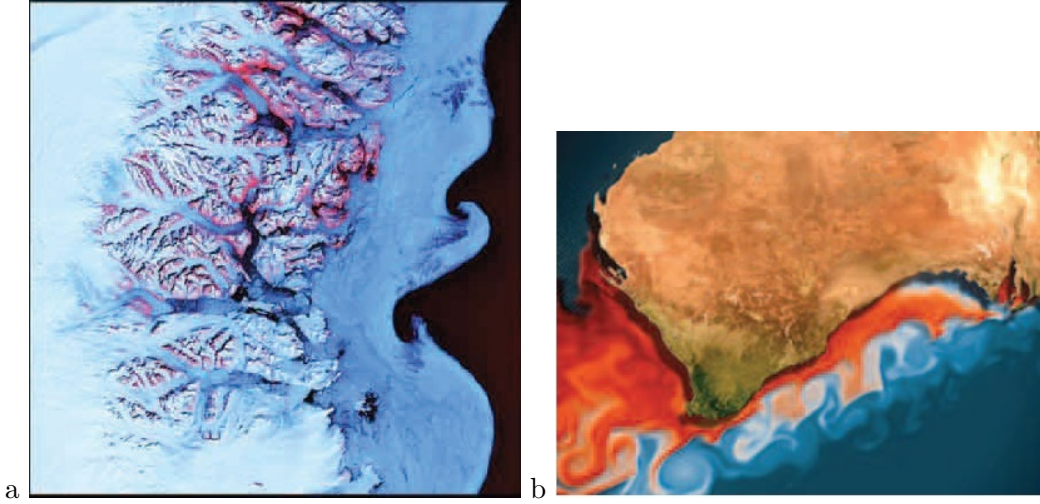$$0 = -\frac{1}{\rho_0}p_z - \frac{g\rho}{\rho_0}, \tag{3}$$

1

Figure 1: Two real-life examples of the effect of the Coriolis force on currents: the East Greenland current flowing in the northerly direction on the Northern hemisphere (a) and the Leeuwin current flowing in the southerly direction near the coast of western coast of Australia on the Southern hemisphere.

where we have assumed that there is no motion in the z direction, that is, we have made the shallow water approximation. The magnitude of the Coriolis force is denoted by $f = 2\Omega$. Conservation of volume is given by:

$$h_t + (uh)_x + (vh)_y = 0. \tag{4}$$

It can be shown (see appendix A) that (1-4) are consistent with the conservation of (shallow water) potential vorticity:

$$q = \frac{f + \zeta}{h} \quad \text{and} \quad \frac{D}{Dt}(q) = 0, \tag{5}$$

where ζ, the relative vorticity, is defined as:

$$\zeta = v_x - u_y. \tag{6}$$

Making the usual hydrostatic assumption, the pressure in the fluid $p(z)$ can be written as:

$$p(z) = \begin{cases} g\rho_U(\eta - z) & -h \leq z \leq \eta, \\ g\rho_U(h + \eta) - g\rho_L(z + h) & z \leq -h, \end{cases} \tag{7}$$

where $\eta = \eta(x, y)$ is the free surface elevation. We are in interested in solutions that are steady. We thus ignore the $\partial/\partial t$ term in addition to the non-linear advective momentum terms in (2), as part of a small-amplitude approximation, and obtain the equation for geostrophic balance between the Coriolis force and the pressure gradient in the direction normal to the axis of rotation:

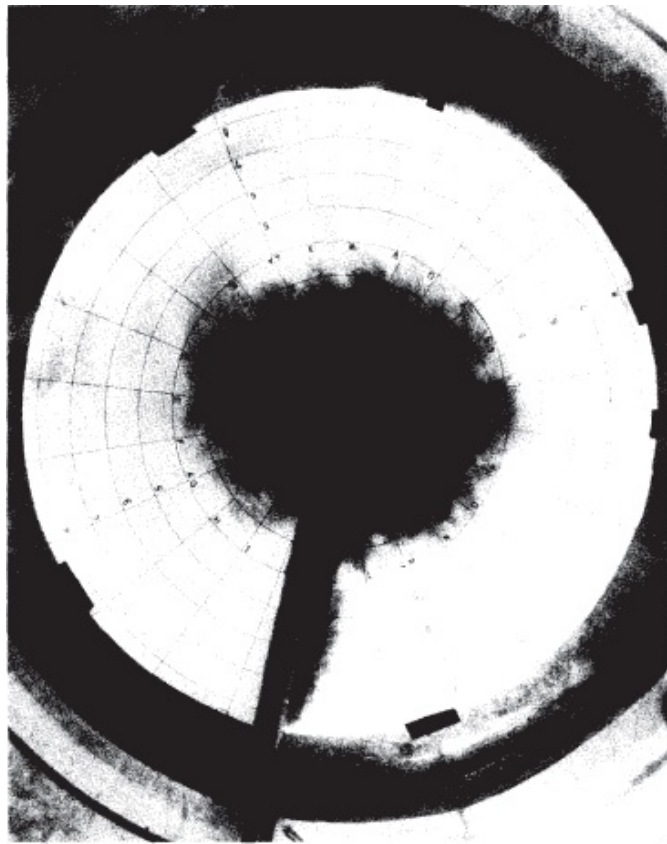$$fu = -\frac{1}{\rho_0}p_y. \tag{8}$$

2

Figure 2: Plan view of a buoyant region of fluid adjusting geostrophically next to a side boundary from [3].

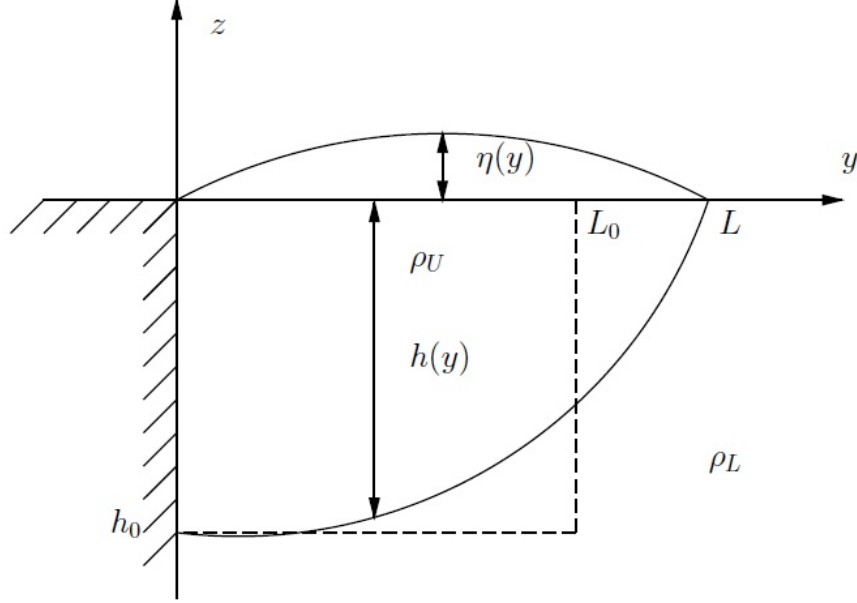Figure 3: A schematic diagram of an idealized dense gravity current in a rotating reference frame.

Combining (7) and (8) gives:

$$\rho_0 fu = \begin{cases} -g\rho_U \frac{\partial \eta}{\partial y} & -h \leq z \leq \eta, \\ -g\rho_U \frac{\partial \eta}{\partial y} + g(\rho_L - \rho_U)\frac{\partial h}{\partial y} & z \leq -h. \end{cases} \tag{9}$$

Now suppose that the lower layer is deep, so that it can be considered passive and its velocity can be ignored. We have from the lower layer part ($z \leq -h$) of (9):

$$-g\rho_U \frac{\partial \eta}{\partial y} + g(\rho_L - \rho_U)\frac{\partial h}{\partial y} = 0. \tag{10}$$

Substituting from (10), the upper layer part ($-h \leq z \leq \eta$) of (9), can now be rewritten as:

$$fu = -g'\frac{\partial h}{\partial y}, \tag{11}$$

where $g' = g(\rho_L - \rho_U)/\rho_0$. Equation (11) holds for the fluid inside the gravity current. From conservation of potential vorticity (5), we have:

$$q = \frac{f}{h_0} = \frac{f - \frac{\partial u}{\partial y}}{h}, \tag{12}$$

where $\partial v/\partial x = 0$, since we ignore all variation in the x-direction, the direction of propagation of the gravity current. Combination of (11) and (12) gives a second-order ordinary differential equation in h

$$\frac{\partial^2 h}{\partial y^2} - \frac{1}{R_D^2}h = -\frac{f^2}{g'}, \tag{13}$$

4

where $R_D = \frac{\sqrt{g'h_0}}{f}$ is the so-called Rossby deformation radius. Physically, this represents the length scale over which the flow starts to experience the effects of rotation.

We can solve the ordinary differential equation (13) assuming the boundary condition $h = 0$ at $y = L$, the right hand side boundary of the gravity current, and $u = 0$ at $y = 0$. The second boundary condition derives from the no-flow boundary condition at the wall ($v = 0$) and from neglecting pressure variations in the x-direction ($\partial p/\partial x = 0$). These conditions along with the momentum equation in the x direction (1) imply $\partial u\, \partial t = 0$. If the current is initially at rest at the boundary ($u(t = 0) = 0$), its horizontal velocity at that location will remain zero. The solution to (13) subject to these boundary conditions is then:

$$\frac{h}{h_0} = 1 - \frac{\cosh\left(y/R_D\right)}{\cosh\left(L/R_D\right)}, \tag{14}$$

or in terms of the horizontal velocity in the x-direction:

$$u = \sqrt{g'h_0}\frac{\sinh\left(y/R_D\right)}{\sinh\left(L/R_D\right)}. \tag{15}$$

Finally, conservation of volume gives the steady-state extent of the current in the y-direction L:

$$\int_0^L h(y)dy = h_0 L_0 \rightarrow \frac{L}{R_D} - tanh\frac{L}{R_D} = \frac{L_0}{R_D}. \tag{16}$$

Figure (4) shows the relationship in (16) and its asymptotic behaviour $L \propto L_0$ for large L_0 ($L_0/R_D \gg 1$).

3   Baroclinic instability

Figures 5 and 6 show the set-up and results for a laboratory experiment exploring the dynamics of a coastal current and the onset of baroclinic instability in these currents. Figure 5 shows a rotating tank with a layer of light fluid initially held in place by an annular lock. The outer wall of the annulus is then removed, and the fluid starts to spread radially, which leads to the formation of an anticyclonic (clockwise) current. Figure 6 shows a top view of the current with the light fluid being dyed. The sequence of figures shows the growth of a baroclinic instability.

Baroclinic instability is a mechanism by which available potential energy is released and converted to kinetic energy. Consider a system shown in figure 7. The solid lines are isopycnals and the dashed lines are geopotentials. There is also a current out of the plane that decreases with height and is thus sheared. The system is in a steady state: the tendency of the isopycnals to become horizontal is balanced by the Coriolis force associated with the shear flow. By differentiating the equation for geostrophic balance (8) with respect to the vertical coordinate z keeping the rate of rotation f constant combined with hydrostatic pressure variation from (3), we obtain:

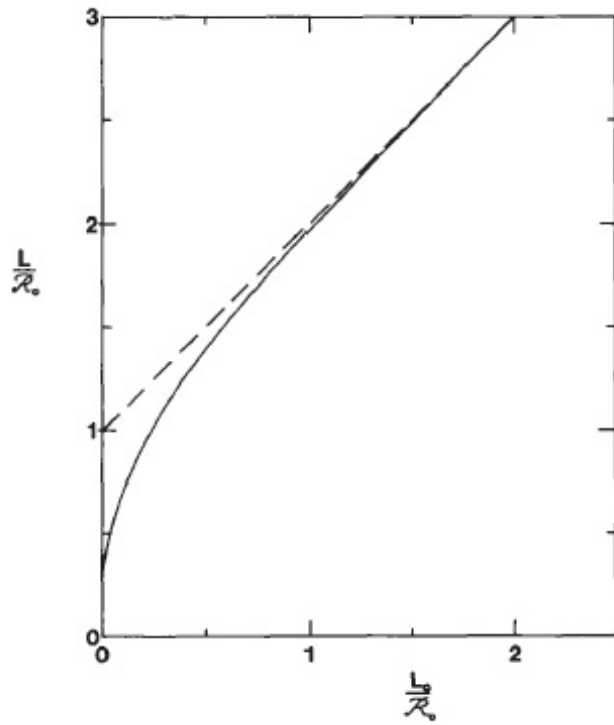$$f\frac{\partial u}{\partial z} = +\frac{g}{\rho_0}\frac{\partial \rho}{\partial y}. \tag{17}$$

Figure 4: The relationship between the initial width L_0 of the upper layer inside the annulus and the final width L in quasi-geostrophic balance. The solid line is given by (16), while the dashed straight line assumes that the edge of the upper layer is directly proportional to L_0. From [1].
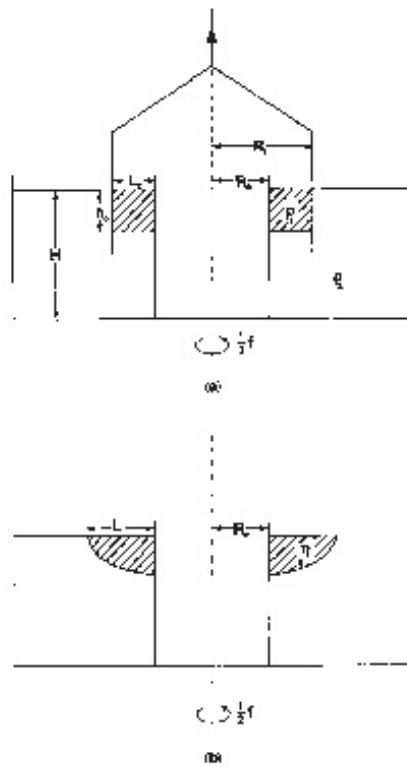
Figure 5: Diagrams of the baroclinic instability experiment before the outer wall of the annulus is withdrawn (a) and after the two layers have adjusted to a quasi-geostrophic balance (b).
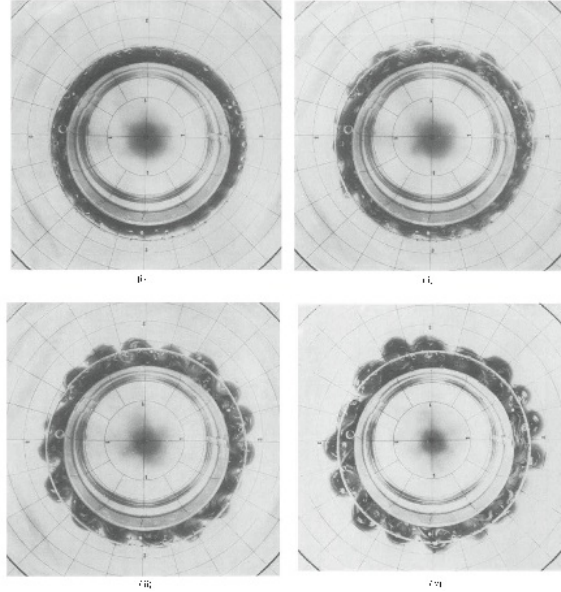
Figure 6: The top view of the baroclinic instability experiment. The panels show the time evolution of the experiment after the outer wall of the annulus is removed. The light fluid is dyed.

The vertical shear is required to satisfy the so-called thermal wind relation (17), in which vertical shear balances horizontal density gradients.

We now examine the stability of this equilibrium to perturbations using figure 7 by considering the available potential energy of the system. We consider three different perturbations. If a parcel of fluid is moved vertically down, it will be surrounded by denser fluid and be restored to its original position by its own buoyancy. If the same parcel is displaced horizontally, buoyancy forces will not act to return the parcel to its initial position, but no potential energy will be released. The perturbation that does release potential energy and does not result in the parcel of fluid being restored to its initial position, is one in which the particle is moved both vertical and horizontally, as illustrated by the arrow in figure 7. This perturbation will grow in size and is called a baroclinic instability. We note that in the figure the vertical scale is exaggerated. In reality the angle between isopycnals and geopotentials is very small, and fluid parcels need to move great horizontal distances to reduce convert their available potential energy into kinetic energy. Consequently, the horizontal scale of baroclinic instabilities is large.

4   Rotating lock exchange

Figure (8) shows the behaviour of a gravity current, as discussed in the previous lectures, but now under the influence of rotation. For each panel (I, II), the subsequent sub-panels (a-
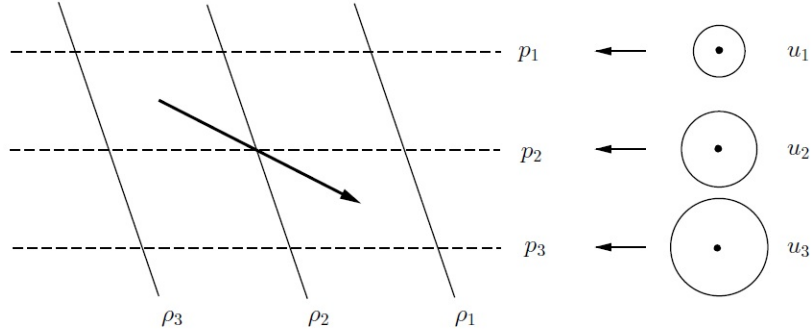
8

Figure 7: A schematic diagram of baroclinic instability in a continuously stratified fluid. The horizontal (dashed) lines denote surfaces of constant pressure (or geopotential) surfaces, where $p_3 > p_2 > p_2$, and the inclined (continuous lines) denote lines of constant density (or isopycnal) surfaces, where $\rho_3 > \rho_2 > \rho_1$. The velocity out of the plane increases with depth ($u_3 > u_2 > u_1$) denoted by circles of increasing radius, and the corresponding shear results in a horizontal torque that is in equilibrium with the horizontal density gradient.

e) show the time evolution of the experiments. The rotation rate is zero in panel I and large for panel II. As the rotation is increased we can see the effect of the Coriolis force, which turns the flow to its right. The flow moves along the right hand side wall of the channel (as seen from the direction of propagation of the current). As the Coriolis is pushing the fluid towards the side wall, it is not able to escape and form a strong front in the same wave a gravity current unaffected by rotation would. The fluid gets trapped in the initial release and can only escape along the wall and forms a boundary current.

A   Conservation of potential vorticity in shallow water

To derive conservation of potential vorticity in shallow water making use of the Boussinesq approximation, start with the momentum equations in vector form:

$$\frac{D\mathbf{u}}{Dt} + \mathbf{f} \times \mathbf{u} = \frac{1}{\rho_0}\nabla p - \mathbf{g}\frac{\rho}{\rho_0}, \tag{18}$$

where $\mathbf{f} = f\hat{\mathbf{k}} = 2\Omega\hat{\mathbf{k}}$ and $\mathbf{u} = (u, v, w)$. In Cartesian coordinates (18) takes the form:

$$u_t + uu_x + vu_y - fv = -\frac{1}{\rho_0}p_x, \tag{19}$$

$$v_t + uv_x + vv_y + fu = -\frac{1}{\rho_0}p_y, \tag{20}$$

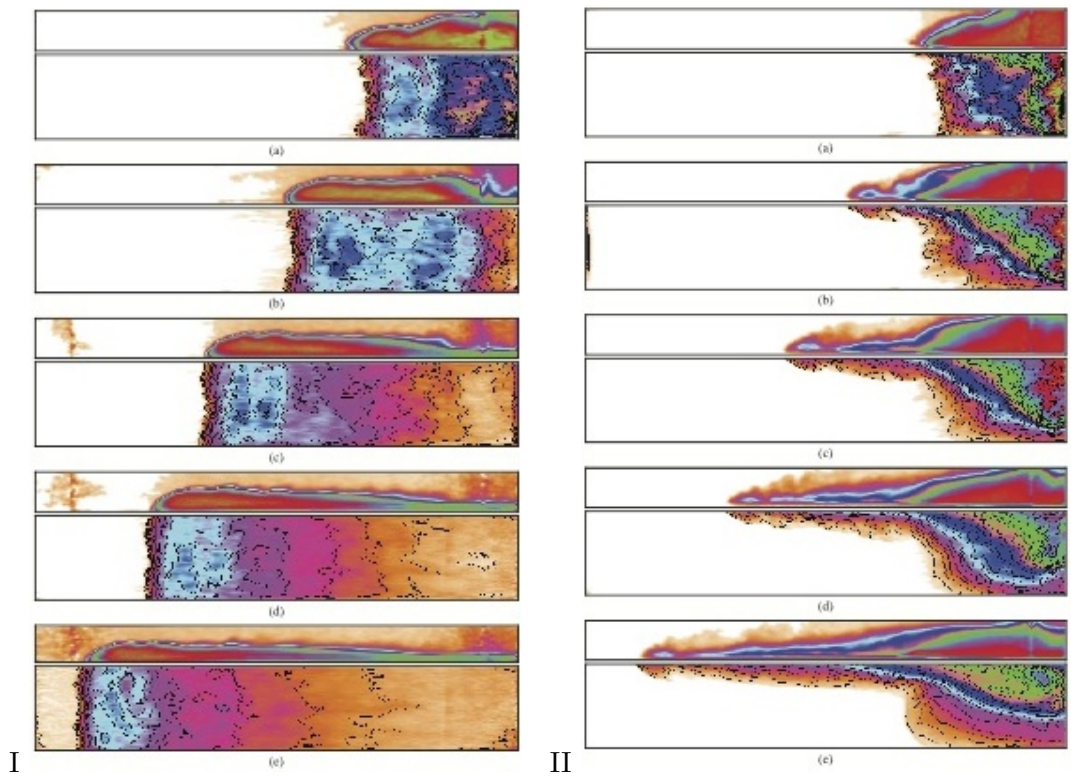$$0 = -\frac{1}{\rho_0}p_z - \frac{g\rho}{\rho_0}, \tag{21}$$

9

Figure 8: Results from two lock-exchange experiments one without rotation (I) and one with strong rotation (II). For each panel (I, II), the sub-panels (a-e) show the time evolution of the experiments. Within each sub-panel, the narrow top section shows the side view and the bottom section shows the top view. From [2].

where it has been assumed that the motion is always in the horizontal plane and thence $w = 0$. Taking the curl of (18) gives the following vector for the right hand side:

$$\left(-\frac{g}{\rho_0}\frac{\partial \rho}{\partial y}, \frac{g}{\rho_0}\frac{\partial p}{\partial x}, 0 \right) \tag{22}$$

For the z-component we thus have for the left hand side:

$$\frac{\partial}{\partial x}\left[v_t + uv_x + vv_y + fu \right] - \frac{\partial}{\partial y}\left[u_t + uu_x + vu_y - fv \right] = 0. \tag{23}$$

We define relative vorticity ζ as follows:

$$\zeta = v_x - u_y. \tag{24}$$

Without making further assumptions, equation (23) can now be simplified to:

$$\frac{\partial \zeta}{\partial t} + \mathbf{u} \cdot (\nabla^* \zeta + f) + (f + \zeta)\nabla^* \cdot \mathbf{u} = 0, \tag{25}$$

which can be written in terms of a material derivative:

$$\frac{D}{Dt}(f + \zeta) + (f + \zeta)\nabla^* \cdot \mathbf{u} = 0. \tag{26}$$

where we have let ∇^* denote the vector differential operator in the x and the y coordinate only: $\nabla^* = \hat{\mathbf{i}}\partial/\partial x + \hat{\mathbf{j}}\partial/\partial y$. From conservation of volume we have:

$$\frac{Dh}{Dt} + h\nabla^* \cdot \mathbf{u} = 0, \tag{27}$$

where h is the depth of fluid. Combining conservation of volume (27) and (26) gives, after multiplication by h, the conserved quantity known as potential vorticity $(f + \zeta)/h$:

$$\frac{D}{Dt}\left(\frac{f + \zeta}{h} \right). \tag{28}$$

References

[1] R. W. GRIFFITHS AND P.F. LINDEN, *Laboratory experiments on fronts*, Geophys. Astrophys. Fluid Dyn., 19 (1982), pp. 159–187.

[2] J. HACKER, *Gravity currents in rotating channels*, PhD thesis, University of Cambridge, 1996.

[3] P. WADHAMS, A. E. GILL, AND P. F. LINDEN, *Transects by submarine of the East Greenland Polar Front*, Deep-Sea Research, 26A (1979), pp. 1311–1327.